10.1 QUALITATIVE AND QUANTITATIVE COMPARISONS OF A BASE-STATE SUBSTITUTION SIMULATION WITH DUAL-DOPPLER OBSERVATIONS OF THE 29 MAY 2012 KINGFISHER SUPERCELL

Casey E. Davenport[*]
University of North Carolina at Charlotte

M.I. Biggerstaff
School of Meteorology, University of Oklahoma

C.L. Ziegler
National Severe Storms Laboratory

1. MOTIVATION

A common approach to understanding the fundamental processes of deep, moist convection has been to utilize idealized numerical simulations. These simulations often employ horizontally- and temporally-homogeneous base-state conditions to isolate the key processes at work, despite knowledge that heterogeneity is inherent in many convective storm environments (e.g., Brooks et al. 1996; Weckwerth et al. 1996; Markowski and Richardson 2007). Much of what we understand about convective storm dynamics arose from idealized simulations that did not include horizontal or temporal variability in the base-state environment (e.g., Klemp 1987). Accounting for environmental heterogeneity in an idealized setting has largely been avoided because of numerous complicating factors that can prevent a clean separation of cause and effect in experimental results. However, it is unknown how the fundamental processes governing severe convection are influenced by changes in the surrounding environment; there is evidence that such processes can be significantly altered (e.g., Davenport and Parker 2015).

Base-state substitution (BSS; Letkewicz et al. 2013) is an idealized modeling method that was designed incorporate the effects of heterogeneity (i.e., changing the base-state) without the complexities of introducing spatial variability. Essentially, BSS approximates the temporal tendencies in temperature, moisture, and wind actually experienced by a storm as it encounters a changing environment. In other words, a new proximity sounding is imposed at a desired rate (see Letkewicz et al. 2013, their Fig. 1). A schematic of the procedure for BSS is shown in Fig. 1 and described in detail in Letkewicz et al. (2013). Briefly, after a certain amount of model run time, BSS separates out the storm-induced perturbations of temperature, moisture, and wind from the original base-state, and then replaces the original horizontally-homogeneous background environment with a new horizontally-homogeneous environment; this is completed at a prescribed temporal interval defined by the model user. This approach permits the user to *independently* modify temperature, moisture, or wind profiles as desired, which provides a significant amount of control over changes to the environment and consequently allows the user to more readily identify cause and effect in their experiments.

The primary assumption of BSS is that the *integrated* effect of a storm moving across an environmental gradient over time is larger than the *instantaneous* effect of local storm-scale gradients. This assumption is central not only to BSS, but to *all* idealized models with horizontally-homogeneous environments employing a representative proximity sounding to the entire domain. The key question is whether this assumption is valid. Will a BSS simulation, employing only temporal variability, produce a realistic storm evolution? To what extent is employing BSS more realistic than not changing the environment at all? To address these questions, idealized simulations with and without BSS will be qualitatively and quantitatively compared to observations of an isolated supercell thunderstorm.

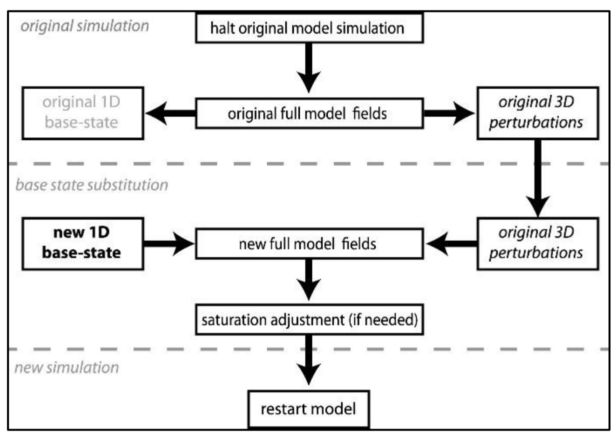

Figure 1: Schematic of the procedure followed for base-state substation. See Letkewicz et al. (2013) for more details.

2. OBSERVATIONS

The Kingfisher supercell thunderstorm, observed on 29 May 2012 during the Deep Convective Clouds and Chemistry field program (DC3; Barth et al. 2015), was chosen due to the availability of extensive observations of the storm as the near-inflow environment evolved. Three soundings (one pre-convective, two near-inflow)

[*] *Corresponding author address*: Casey E. Davenport, University of North Carolina at Charlotte, Department of Geography and Earth Sciences, Charlotte, NC 28223; email: Casey.Davenport@uncc.edu

were launched over the lifetime of the storm, at 2029, 2255, and 0020 UTC, capturing notable modifications to thermodynamic and kinematic profiles (Fig. 2; Table 1). Overall, CAPE increased over time, CIN remained about the same, but both 0-3 km SRH and BRN shear significantly increased. The combination of these environmental changes would support a more intense rotating storm, which was indeed what was observed (Fig. 3).

Multiple-Doppler data was collected between 2251 and 0000 UTC, providing key observations of storm structure over an extended period of time, within which the surrounding environment underwent significant changes. Three mobile radars collected coordinated scans of the Kingfisher storm: the two SMART-Rs (Biggerstaff et al. 2005) and the NOXP radar (Burgess et al. 2010). Time synced radar volumes were collected every three minutes by all three radars, however the storm was never located in the triple-Doppler region. Wind retrieval was achieved using the variational method described in Potvin et al. (2012). A nearby environmental sounding provided the background field for the analysis, which was then blended with the storm using a low-pass filter. Each radar volume was interpolated to a 90 x 60 x 17.5 km Cartesian grid using natural neighbor interpolation (Ledoux and Gold 2005). The horizontal and vertical grid spacing was 500 m.

3. MODEL EXPERIMENTS

The idealized numerical model CM1 (Bryan and Fritsch 2002), release 18, was utilized for the modeling component of this study. The domain was 300 x 400 x 21 km, with a horizontal grid spacing of 500 m (same as the observations) and a stretched vertical grid (100 m near the model surface to 500 m aloft). Convection was initiated using moist convergence (relative humidity

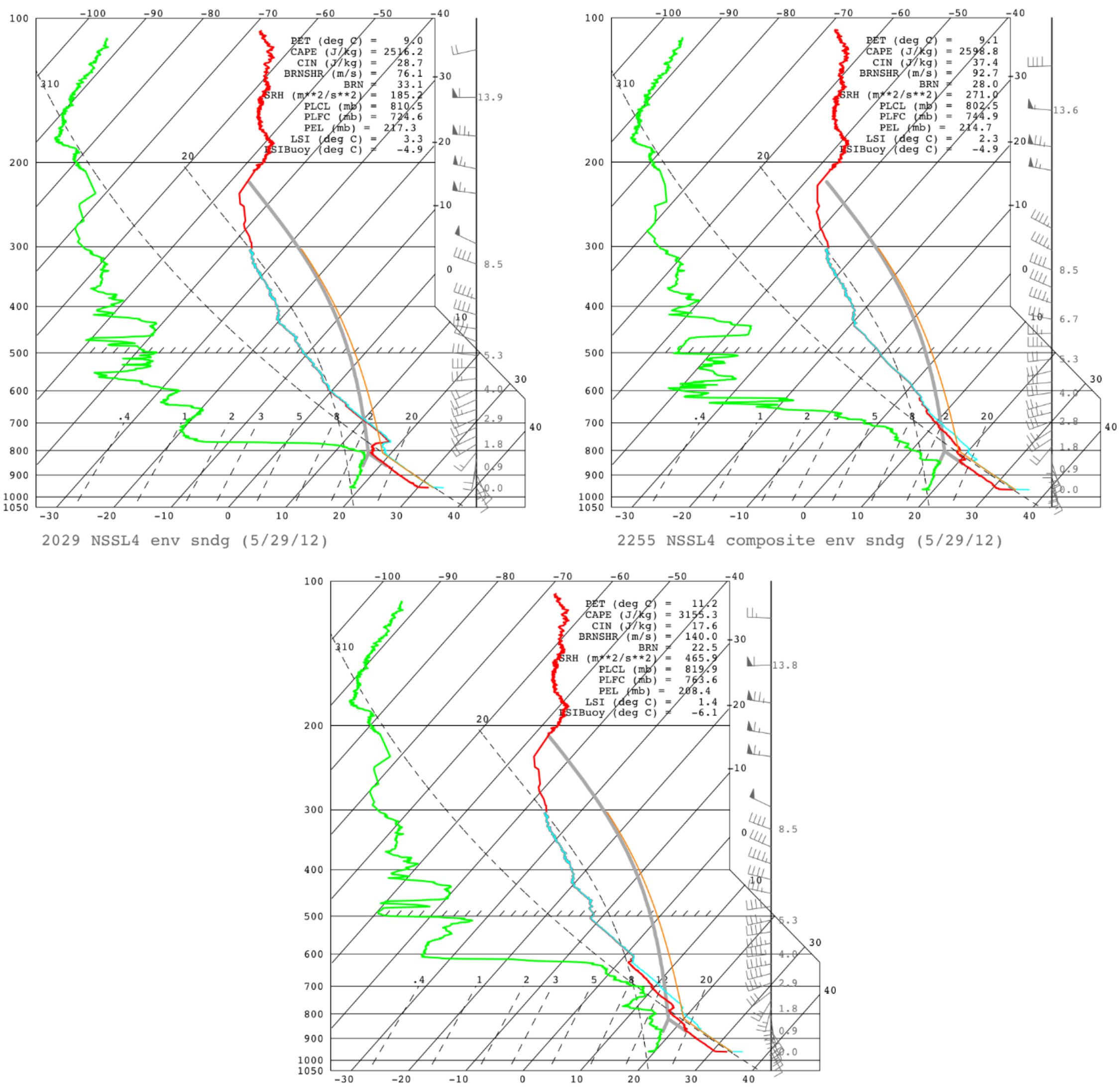

Figure 2: Skew-T log-p diagrams of observed inflow soundings from DC3 experiment on 29-30 May 2012.

Parameter	2029 UTC	2255 UTC	0020 UTC
CAPE (J/kg)	2516	2599	3155
CIN (J/kg)	-29	-37	-18
0-3 km SRH (m^2/s^2)	185	271	466
BRN Shear (m/s)	76	93	140

Table 1: Evolution of select thermodynamic and kinematic parameters associated with the soundings launched on 29-30 May 2012; cf. Fig. 2.

initially set at 95% within the zone of convergence; Loftus et al. 2008) over the first 30 min of the simulation. Microphysics were governed by the National Severe Storm Laboratory's double moment variable graupel and hail density scheme (Mansell et al. 2010).

The observed soundings were utilized to describe the horizontally-homogeneous base-state environment in the model and were incorporated into the simulations via the BSS technique. Note that in this study, the BSS approach has been updated to occur every time step before the model is integrated forward (hereafter "continuous BSS"); no model restarts are needed. In other words, a tendency is applied to base-state variables based on the differences between the input soundings. The perturbations of temperature, moisture, and wind are still retained as before.

Convection was observed to initiate around 2130 UTC on 29 May; to approximate this environment in the model, a linear interpolation was performed between the 2029 UTC and 2255 UTC profiles. Slight moistening was required (5% RH in the lowest 4 km) in order to achieve long-lived convection in the model. This slightly moistened environment thus represented the original base-state in the model; the control simulation maintained this background environment for the entirety of the simulation (5 hours). In the BSS simulation, the base-state temperature, moisture, and wind profiles were continuously modified to the 2255 and 0020 UTC profiles once an isolated supercell developed, starting at 135 min into the simulation. Note that to maintain the same observed change in moisture, the 2255 and 0020 UTC profiles were also slightly moistened; utilizing these slightly modified profiles did not impact the results.

3. QUALITATIVE COMPARISONS

An overview of the simulation results in comparison to the observations is shown in Fig. 3. It is evident in both the control and BSS simulations that long-lived supercells are produced, though their evolutions during the observation period (2251 UTC corresponds to approximately 3.5 hours into the simulations) are quite different. Note that the observed supercell's updraft grew larger over time. In contrast, the control simulation's updraft grew smaller, and the size of the storm overall also appears to shrink. The BSS supercell, on the other hand, grows in size, as does its updraft.

Time-height plots of maximum vertical velocity and maximum vertical vorticity further reveal differences in the evolutions of the observed and simulated supercells.

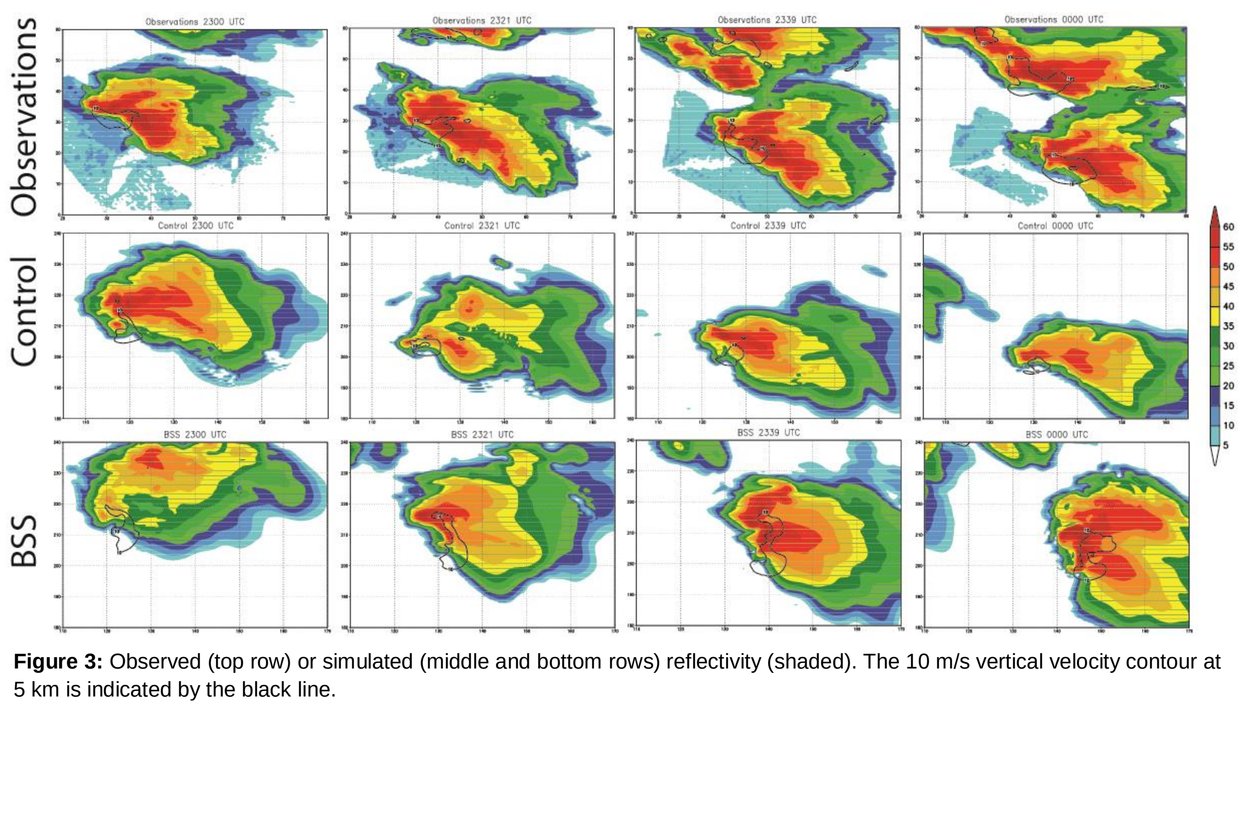

Figure 3: Observed (top row) or simulated (middle and bottom rows) reflectivity (shaded). The 10 m/s vertical velocity contour at 5 km is indicated by the black line.

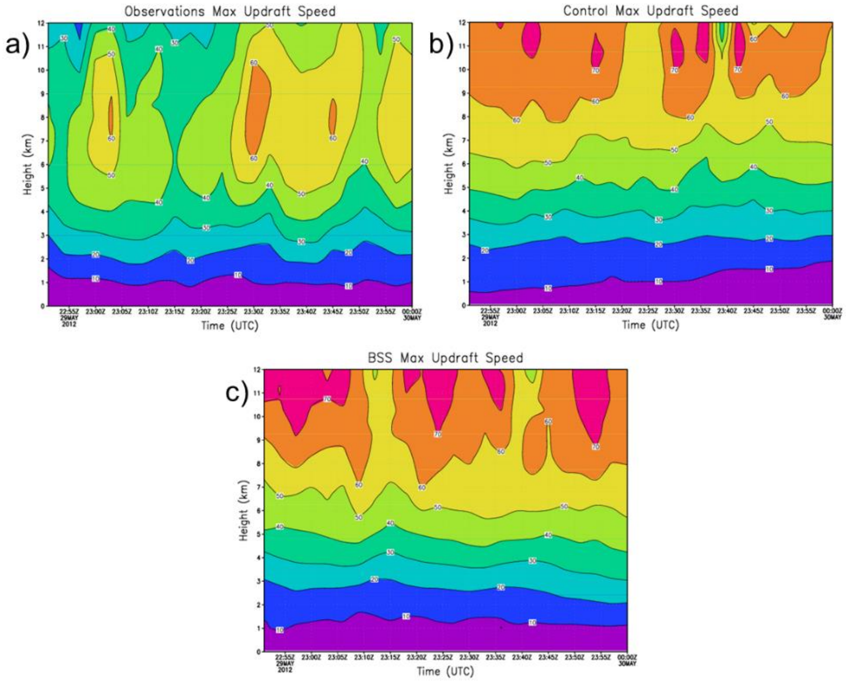

Figure 4: Time-height plots of maximum vertical velocity in the a) observed, b) control, and c) BSS supercells.

In the observed supercell, the updraft is strongest between approximately 6-10 km; the main trend of note is a general increase in the maximum intensity of the updraft over time, especially after 2330 UTC (Fig. 4a). In the simulations, the structure and intensity of maximum velocity is quite different, in that the strongest speeds are in the upper-levels of the storm, above 10 km, and are much more intense than the observations. While this is a notable deviation from the observations, the trends in the control and BSS simulations are nevertheless dissimilar. Over time, the strongest vertical velocities weaken in the control simulation; this is particularly evident in the low-levels (~1 km) and upper-levels (~10-12 km; Fig. 4b). In contrast, the velocities intensify over time in the BSS simulation, particularly throughout the lowest 5 km of the storm (Fig. 4c). Thus, even though the structure and magnitude is different, the BSS supercell better reflects the overall trends observed in the Kingfisher supercell. A similar conclusion can be reached through examination of time-height plots of maximum vertical vorticity (Fig. 5).

4. QUANTITATIVE COMPARISONS

Qualitative comparisons of reflectivity provide a useful first-glance at how the simulations compare to the observations, but to fully assess the ability of BSS to produce realistic results, we wish to probe deeper with quantitative and statistical comparisons. We first examine how the area of the updraft (defined as velocities $\geq$ 5 m/s) evolved over time throughout the depth of the storm. As evident in Fig. 6a, the observations clearly show a growing updraft over time; the updraft is largest in the mid-levels, consistent with the time-height plot of maximum vertical velocity (cf. Fig. 4a) and the environment's increase in CAPE and SRH, supporting a more intense storm. The simulations again have a different structure (larger updraft areas at a higher

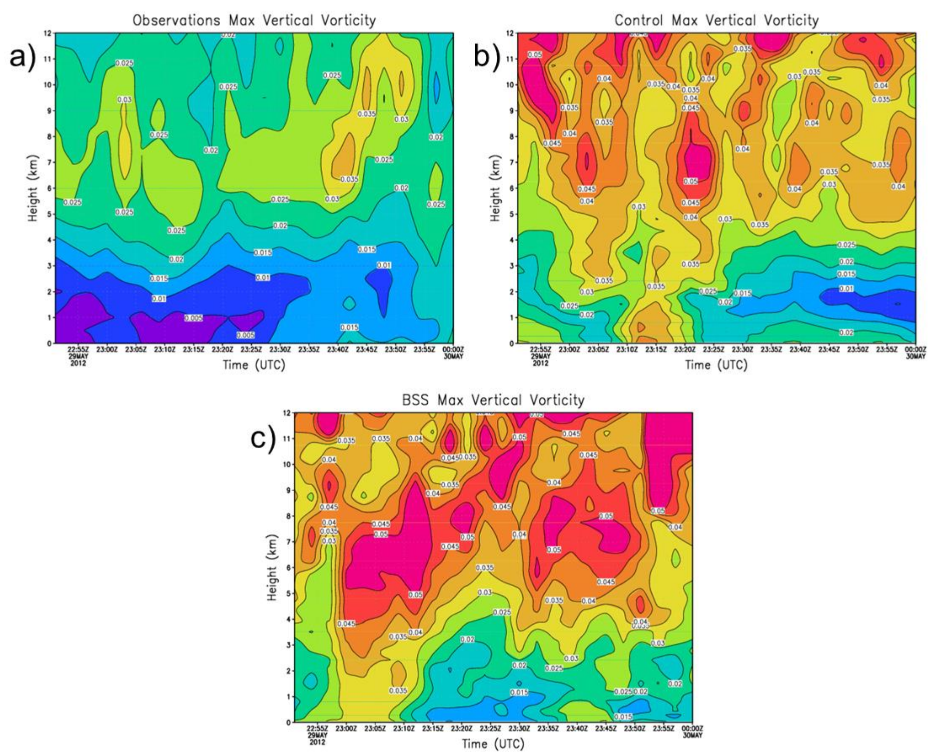

Figure 5: As in Fig. 4, but for maximum vertical vorticity. .

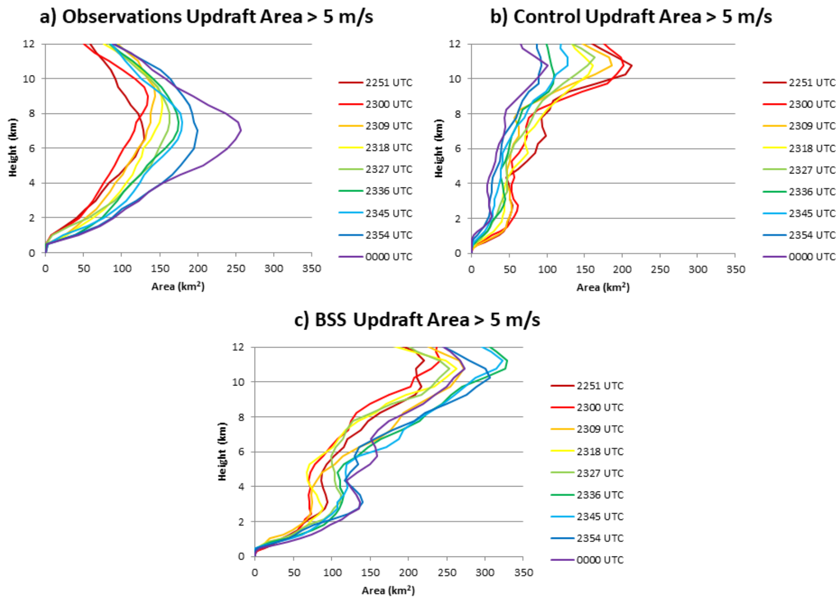

Figure 6: Vertical profiles of the area of the updraft (velocities $\geq$ 5 m/s) throughout the depth of the storm in the a) observations, b) control simulation, and c) BSS simulation.

altitude), but the trends differ. The control simulation clearly shows a shrinking updraft over time at all levels (Fig. 6b), while the BSS simulation contains an updraft increasing in size (Fig. 6c). This comparison also holds true when focusing on the size of the most intense velocities ($\geq$ 20 m/s; Fig. 7).

We also compare trends in the areas of cyclonic rotation, defined here as vertical vorticity $\geq$ 0.01 s^{-1}, approximating the size of the mesocyclone. In the observations, there is not as clear of an increase in the size of the mesocyclone over time, but it does enlarge slightly in the mid-levels (Fig. 8a). The control simulation trend is quite different, with significant shrinking of the rotational area throughout the low-, mid-, and upper-levels (Fig. 8b). The mesocyclone in the BSS simulation does increase in size more significantly than the observations, but its trend is at least in the same direction (Fig. 6c).

In addition to comparisons of trends in rotation and updraft areas, we also took a statistical approach to quantifying the degree of similarity between the observations and each simulation. This is achieved by first computing distributions of vertical velocity and vertical vorticity every 500 m in the observations and both simulations (a linear interpolation was performed to determine values at the same altitudes as the observations). These distributions were limited to a 35 x 35 km box surrounding the storm; an example distribution is shown in Fig. 9. Next, the non-parametric two-way Kolmogorov-Smirov (KS) test was used to determine the similarity of the distributions at each vertical level. Comparisons are made between the observations and the control simulation, as well as the observations and the BSS simulation. The KS test quantifies the distance between the empirical distribution functions of the two sample distributions; the null hypothesis is that the two samples are drawn from the same distribution. Thus, a small p-value (close to zero) indicates that the two samples are likely drawn from *different* distributions, while a large p-value (close to one) indicates that the two samples are likely drawn from the *same* distribution.

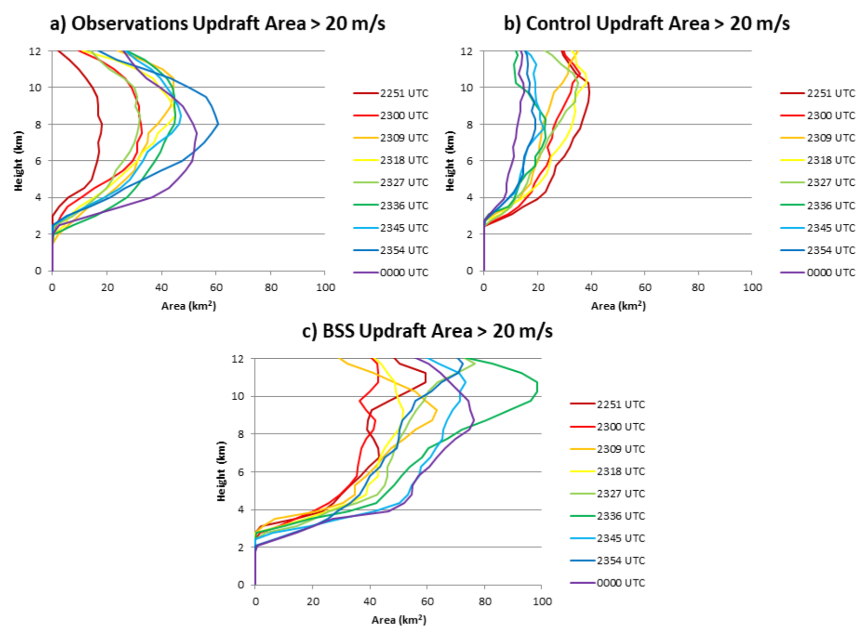

Figure 7: As in Fig. 6, but for velocities $\geq$ 20 m/s.

Vertical profiles of p-values were examined throughout the analysis period; unfortunately, these profiles were

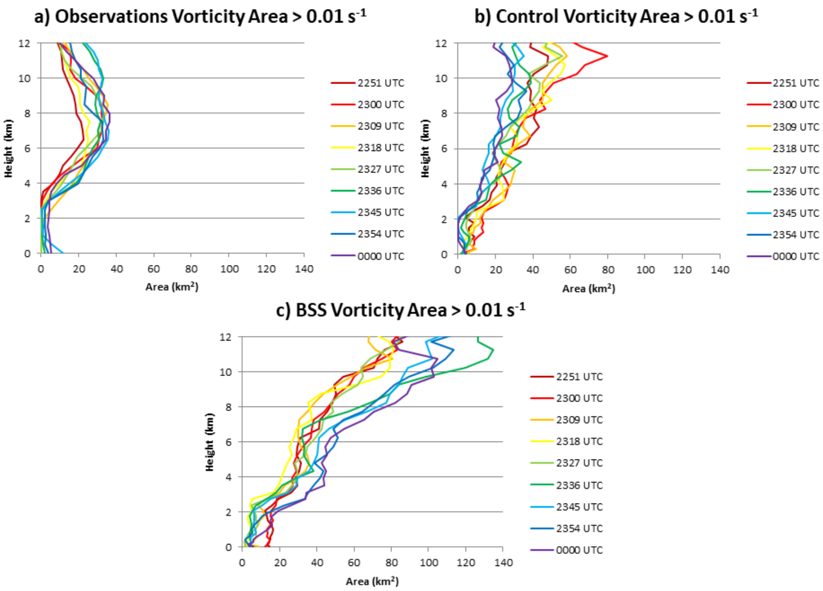

Figure 8: As in Fig. 6, but for vertical vorticity $\geq 0.01\ s^{-1}$.

quite noisy, and the trends difficult to clearly identify at times (thus not shown). However, broadly speaking, distributions of vertical velocity in the BSS simulation were increasingly similar to the observations, while distributions of vertical vorticity in the control simulation were increasingly similar to the observations. The latter result was somewhat surprising, but as Fig. 9 suggests, it appears that this was likely due to the fact that the control simulation was weakening over time; since the simulated vertical vorticity was much larger in magnitude than the observations (cf. Fig. 5), as the storm weakened, its values became more in line with the observations.

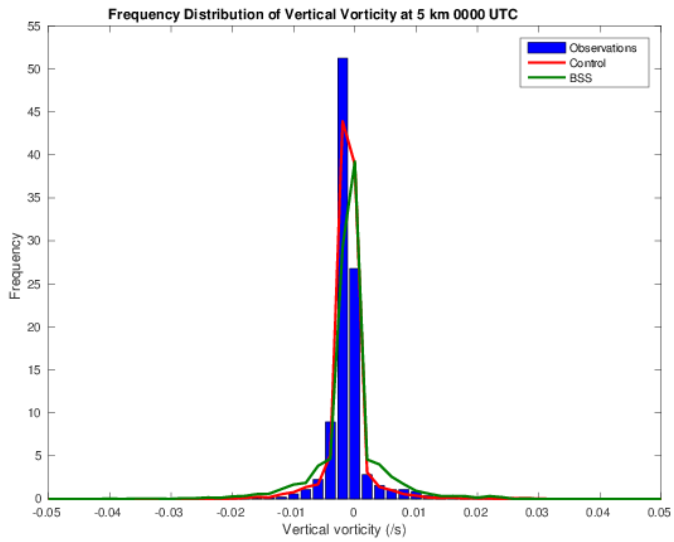

Figure 9: Frequency distributions of vertical vorticity at 5 km at 0000 UTC. Observations are shown in blue, control in red, and BSS in green.

5. SUMMARY AND FUTURE WORK

Base-state substitution is a useful approach to accounting for the effects of environmental variability in an idealized setting while still maintaining a large degree of control over the simulations. However, it is unknown the extent to which a realistic storm is produced or a realistic evolution results. Given the idealized context, how much more realistic is a storm produced via BSS than one produced in a simulation without any environmental changes? Broadly speaking, to what extent does a series of representative inflow soundings accurately reflect observed storm evolution?

To address these questions, comparisons were made between multiple-Doppler observations of the Kingfisher supercell storm and two idealized simulations of it, one with shifts in the background environment and one without. Qualitatively, the BSS supercell better replicated the intensifying trend of the observed supercell (Figs. 3-5). This was confirmed with a variety of quantitative comparisons, including the size of the updraft and rotation areas (Figs. 6-8). Statistical comparisons using the two-way KS test were less conclusive, due to the notable different simulated structures in the vertical, and different magnitudes. Nevertheless, overall, BSS represents a more realistic idealized approximation of the Kingfisher supercell, and is a notable improvement over the control simulation where the background environment remained unchanged.

Additional work is needed to produce simulated storm structures and magnitudes more in line with the observations; one such avenue will be to tweak the entrainment rate in the model. Beyond some modifications to the model set-up, we also intend to further quantify the degree of similarity among the simulations and observations by utilizing spatial statistics. Finally, we also plan to assess the sensitivity of our results to factors such as the choice of microphysical parameterization.

6. REFERENCES

Barth, M.C., and Coauthors, 2015: The Deep Convective Clouds and Chemistry (DC3) Field

Campaign. *Bull. Amer. Meteor. Soc.*, **96**, 1281—1309.

Biggerstaff, M.I., and Coauthors, 2005: The Shared Mobile Atmospheric Research and Teaching Radar: A Collaboration to Enhance Research and Teaching. *Bull. Amer. Meteor. Soc.*, **86**, 1283—1274.

Brooks, H.E., C.A. Doswell III, M.T. Carr, and J.E. Ruthford, 1996: Preliminary analysis of VORTEX-95 soundings. NOAA/NSSL, 133 pp.

Bryan, G.H., and J M. Fritsch, 2002: A benchmark simulation for moist nonhydrostatic numerical models. *Mon. Wea. Rev*., **130**, 2917—2928.

Davenport, C.E., and M.D. Parker, 2015: Impact of environmental heterogeneity on the dynamics of a dissipating supercell thunderstorm. *Mon. Wea. Rev.*, **143**, 4244—4277.

Klemp, J.B., 1987: Dynamics of tornadic thunderstorms. *Ann. Rev. Fluid Mech.*, **19**, 369—402.

Letkewicz, C.E., A.J. French, and M.D. Parker, 2013: Base-state substitution: An idealized modeling technique for approximating environmental variability. *Mon. Wea. Rev.*, **141**, 3062—3086.

Loftus, A. M., D. B. Weber, and C. A. Doswell III, 2008: Parameterized mesoscale forcing mechanisms for initiating numerically simulated isolated multicellular convection. *Mon. Wea. Rev*., **136**, 2408–2421.

Mansell, E. R., C. L. Ziegler, and E. C. Bruning, 2010: Simulated electrification of a small thunderstorm with two-moment bulk microphysics. *J. Atmos. Sci*., **67**, 171–194.

Markowski, P., and Y. Richardson, 2007: Observations of vertical wind shear heterogeneity in convective boundary layers. *Mon. Wea. Rev*., **135**, 843—861.

Potvin, C.K., Shapiro, A., and M Xue, 2012: Impact of a Vertical Vorticity Constraint in Variational Dual-Doppler Wind Analysis: Tests with Real and Simulated Supercell Data. *J. Atmos. Oceanic Techol.*, **29**, 32—49.

Weckwerth, T.M., J.W. Wilson, and R.M. Wakimoto, 1996: Thermodynamic variability within the convective boundary layer due to horizontal convective rolls. *Mon. Wea. Rev.*, **124**, 769—784.